

protein coordinates from a map the connectivity has to be based on atom types rather than on interatomic distances. This program makes the connexions between atoms on the basis of the atom label and at the same time assigns for each connexion a code number which defines the target bond length. Where an atom has more than one connexion the combination of these codes defines the target angle. In a similar way atoms which should be planar are listed and coded. The program calculates bond lengths and angles and prints a list of these which should be checked before the fitting calculations are carried out.

Copies of the Fortran text of this program, which includes the dimensions which we have used for the various standard groups, can be obtained from one of us (N.W.I.).

Conclusions

The method of this paper has invariably produced models for protein structures with acceptable bond lengths, bond angles, and planarities, and the positions obtained have fitted all the atomic positions derived from refinement processes, within the limits prescribed on the basis of the estimated accuracies of these positions. The cost of applying the method has been considerably less than that of computing a difference map or that for the corresponding set of structure factors, in the case of insulin. Since the starting model need not obey the constraints accurately, there is no dif-

ficulty in providing suitable starting coordinates, nor in obtaining sufficient convergence from them. The method therefore turns out to be simple to use and free from characteristics which tend to cause failures. This is in a great measure due to the possibility of generating the elements of the observational equations automatically.

The simplicity, power, economy and reliability of the method encourage us to recommend it for general use in protein structure refinement. In combination with methods such as that of Sayre (1972) for generating Fourier maps displaying near atomic resolution, it appears to offer a route to optimally refined models of proteins which requires less tedious precise human interpretation of electron density maps than has been needed up to now.

References

- DIAMOND, R. (1966). *Acta Cryst.* **21**, 253–266.
 HERMANS, J. & MCQUEEN, J. E. (1974). *Acta Cryst.* **A30**, 730–739.
 HESTENES, M. R. & STIEFEL, E. (1952). *J. Res. N.B.S.* **49**, 409–436.
 KENNARD, O., WATSON, D. G. & TOWN, W. G. (1970*a, b*, 1971, 1973, 1974). *Molecular Structures and Dimensions*, Vol. 1 to 5. Utrecht: Oosthoek, Scheltema & Holkema.
 LEVITT, M. (1974). *J. Mol. Biol.* **82**, 393–420.
 LEVITT, M. & LIFSON, S. (1969). *J. Mol. Biol.* **46**, 269–279.
 SAYRE, D. (1972). *Acta Cryst.* **A28**, 210–212.

Acta Cryst. (1976). **A32**, 315

The Temperature Dependence of the Integrated X-ray Diffracted Intensities from Sodium Metal

BY D. W. FIELD AND B. BEDNARZ

Department of Physics, University of Adelaide, North Terrace, Adelaide, South Australia, 5001

(Received 11 August 1975; accepted 27 September 1975)

The temperature dependence of the integrated X-ray diffracted intensities in sodium metal has been determined for the 222, 400, 330, 411 and 332 reflexions in the temperature range 148 K to the melting point of 371 K. In the temperature range 148 K to about 300 K, all the data can be fitted using a quasi-harmonic approximation for the temperature factor. From room temperature to the melting point the intensities for all the reflexions were observed to decrease rapidly with temperature, and could not be fitted either with a quasi-harmonic or fourth-order anharmonic model for the temperature factor. There is no evidence for anisotropy in the intensities below room temperature, but from 293 K to the melting point, anisotropy increases rapidly. A qualitative explanation of the high-temperature phenomena in terms of a lattice relaxation around the vacancies has been advanced.

Introduction

Anisotropy in the room-temperature X-ray structure factors of body-centred cubic sodium has been reported recently (Field & Medlin, 1974, hereinafter referred to as I). In that paper, the integrated intensity data was analysed, following the formalism of Willis (1969), in terms of an anharmonic temperature factor derived from a fourth-order anisotropic expansion of

the single-atom potential function appropriate to the body-centred cubic structure. No conclusion could be drawn from the single-temperature experiment about the contribution of possible isotropic anharmonic terms to the temperature factor because the isotropic parameters are strongly correlated with the harmonic parameters in the least-squares analysis. The experiment discussed in the present paper was carried out to investigate both the possible contribution of isotropic

anharmonic components to the temperature factor and also the temperature dependence of the anisotropy.

Experimental

An ~ 0.3 mm diameter cylindrical single crystal of sodium was grown under paraffin oil in a thin-walled glass capillary tube by a technique described in I. The crystal was oriented about a [110] rotation axis and integrated intensity measurements were made for reflexions on the zero layer on a Stoe two-circle diffractometer. The graphite-monochromated radiation used was at the Mo $K\alpha$ wavelength. The reflexions were step-scanned in ω - 2θ mode. A total of 200 integrated intensities were measured for 10 independent reflexions in the temperature range from 148 K to the melting point of 371 K. These 200 data points were each the average of two measurements under the same conditions. The lower bound of the temperature range used was chosen because at lower temperatures the crystal showed signs of thermal shock, which results in an increase in mosaic spread, and ultimately, disintegration of the crystal into a polycrystalline sample.

The statistical counting errors were kept as small as possible consistent with the demands of time and temperature control. Of the total of 400 measurements, there were 235, 142, 15 and 8 with statistical errors of 0–1%, 1–2%, 2–3% and 3–10% respectively. In general, the larger errors occurred for higher-order reflexions and higher temperatures.

The low-temperature apparatus used was standard Stoe equipment capable of producing crystal temperatures as low as liquid-nitrogen temperature. The crystal was cooled to the desired temperature by an air stream which had been passed through heat-exchanging coils in a dewar of liquid nitrogen. The rate of flow determined the temperature, which was monitored by a chromel–alumel thermocouple tip placed in the air stream about 1 cm in front of the crystal. Gas-flow control was by an on–off valve, switched from the thermocouple output, a large pressurized container to act as a mechanical buffer against surges in gas flow, and needle valves. The precision of the temperature control was ~ 1 K. The same apparatus was converted for use in the temperature range 293 K to 371 K by using heat-exchanging coils in an oven to provide a warm-air flow.

Integrated intensities were measured for all symmetry-related reflexions for all hkl types on the zero layer up to 422 at 198 K, 293 K and 353 K. At other temperatures, the intensity of one reflexion for each hkl type was measured.

Theory

The general expression for the structure factor $F(hkl)$ for allowed reflexions hkl for b.c.c. sodium is given by

$$F(hkl) = 2f(hkl)\tau(hkl)$$

where $f(hkl)$ represents the atomic scattering factor and $\tau(hkl)$ represents the temperature factor.

An expression for the temperature factor taking into account isotropic and anisotropic anharmonic terms to fourth order is given by (Willis & Pryor, 1975)

$$\begin{aligned} \tau(hkl) &= N \exp \left[- \frac{8\pi^2(h^2 + k^2 + l^2)k_B T}{a^2 \alpha} \right] \left\{ 1 - 15k_B T \left[\frac{\gamma}{\alpha^2} \right] \right. \\ &+ 10(k_B T)^2 \left(\frac{2\pi}{a} \right)^2 \left[\frac{\gamma}{\alpha^3} \right] (h^2 + k^2 + l^2) \\ &- (k_B T)^3 \left(\frac{2\pi}{a} \right)^4 \left[\frac{\gamma}{\alpha^4} \right] (h^2 + k^2 + l^2)^2 \\ &\left. - (k_B T)^3 \left(\frac{2\pi}{a} \right)^4 \left[\frac{\delta}{\alpha^4} \right] (h^4 + k^4 + l^4 - \frac{3}{2}(h^2 + k^2 + l^2)^2) \right\} \end{aligned} \quad (1)$$

where

$$N = \left\{ 1 - 15k_B T \left[\frac{\gamma}{\alpha^2} \right] \right\}^{-1},$$

T represents the temperature and α, γ, δ are coefficients in the single-atom potential given by

$$V(u_1, u_2, u_3) = V_0 + \frac{1}{2}\alpha r^2 + \gamma r^4 + \delta(u_1^4 + u_2^4 + u_3^4 - \frac{3}{2}r^4),$$

where

$$r^2 = u_1^2 + u_2^2 + u_3^2$$

and the other symbols have their usual meaning. The temperature dependence of α is taken into account as

$$\frac{1}{\alpha} = \frac{1}{\alpha_0} (1 + 2\gamma_G \chi T) \quad (2)$$

to allow for the ‘softening’ of the vibrations at higher temperature due to thermal expansion. In equation (2), α_0 is temperature invariant, γ_G is the Gruneisen parameter and χ the volume expansion coefficient. In this paper, the temperature dependence of the other potential parameters has been ignored. The value of γ_G used throughout was 1.25, taken from Geshko, Kushta & Mik’halchenko (1968).

Data analysis

The measured integrated intensities were corrected for Lorentz–polarization, anomalous dispersion and thermal diffuse scattering (TDS) effects. Absorption corrections were negligible for a crystal of sodium at Mo $K\alpha$ wavelength. Since sodium is elastically anisotropic, the TDS correction used was the first-order correction of Rouse & Cooper (1969), which takes into account such anisotropy. The variation of the elastic constants with temperature was included in the calculation. The elastic-constant data used were taken from Martinson (1969) for the temperature range 148 to 300 K, and from Fritsch, Geipel & Prasetyo (1973) for the temperature range 300 to 371 K.

The best value of lattice parameter at 273 K was taken to be 4.2811 Å, interpolated from Feder & Charbnau (1966). Values of the lattice parameter at other temperatures were taken from Feder & Charbnau for temperatures from 273 to 371 K, and were evaluated from the above value at 273 K and the expansion data of Siegel & Quimby (1938) for temperatures from 148 to 273 K.

Values of the free-atom scattering factors $f(hkl)$ were generated from the nine-parameter-fit tables of Doyle & Turner (1968) calculated from relativistic Hartree-Fock wave functions. Explicit account was taken of the variation of scattering factor with temperature due to the variation of scattering angle with temperature as a result of expansion. Further, account was taken of the lattice parameter variation with temperature in the expression (1) for temperature factor. These two effects are normally neglected as being small, but they may not be negligible if small deviations of the experiment from the model are being sought. For example, for the 332 reflexion for sodium, the variation over the temperature range of 148 to 371 K of the lattice parameter a , $\sin \theta/\lambda$, $f(hkl)$ and the harmonic part of the temperature factor, $\tau_{\text{harm}}(hkl)$, are ~ 1 , ~ 1 , ~ 1 and $\sim 5\%$ respectively. It is interesting that the variations in the last two quantities are in the opposite sense to any variations expected from changes in the vibration spectrum with temperature. That is, an increase in lattice parameter with temperature gives an increase in $f(hkl)$ and $\tau_{\text{harm}}(hkl)$.

The data were analysed by minimizing the quantity

$$S = \sum_i \omega_i (I_{oi} - I_{ci})^2 \quad (3)$$

where I_{oi} represents the i th corrected observed intensity and I_{ci} represents the i th calculated intensity given by $I_{ci} = KF_{ci}^2$ where K is the scaling factor. The weighting factors ω_i used in equation (3) were given by $\omega_i = 1/\sigma_i^2$ where σ_i was the estimated error in the i th intensity. The σ_i were taken to be 2% of I_{oi} for all reflexions

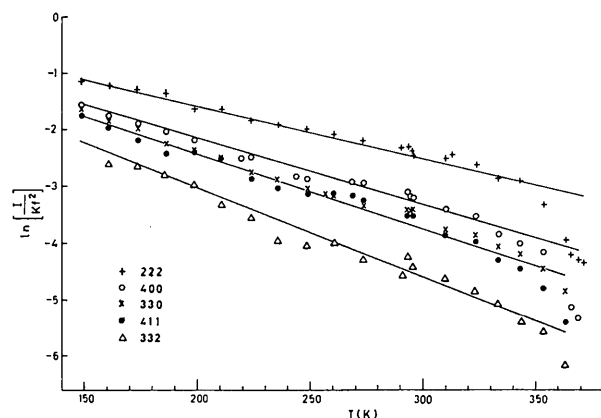


Fig. 1. The variation of $\ln [I_{oi}/Kf^2]$ with temperature for the 222, 400, 330, 411 and 332 reflexions. The value of parameter R is 0.128.

where the statistical counting error was $\sim 1\%$, in order to account for the error due to the estimated 1 K uncertainty in temperature. The figure of 2% was about the average standard error of the mean of the intensities of symmetry-related reflexions at those temperatures (198, 293 and 353 K) where symmetry-related reflexions were measured. Where the statistical counting error was greater than 2% of I_{oi} , the σ_i were taken to be the statistical errors.

Of the 200 averaged measured intensities, 108 were retained in the analysis. Sodium exhibits heavy extinction in the lower-order reflexions; indeed, room-temperature annealing may be observed over a few hours, and we have not been able to use any mathematical procedure to correct the measured intensities for extinction. Those measurements for lower-order reflexions which could not be fitted, owing to extinction, with the rest of the data were discarded. The highest-order reflexion measured, 422, was excluded also from the final analysis. The integrated intensities were consistently too low at all temperatures for 422 to be fitted with the rest of the reflexions. We have taken this to be due to a multiple-reflexion effect. A computation of the position of every other reciprocal-lattice point with respect to the Ewald sphere with 422 in the reflecting position for a b.c.c. crystal rotating about a [110] axis has shown that two 330-type and two 211-type reciprocal lattice points are exactly and simultaneously on the Ewald sphere with the 422 point. The reflexions retained in the final analysis for the whole temperature range were 222, 400, 330, 411 and 332, with one measurement of 220 averaged over all the symmetry-related reflexions at 198 K.

Results

A plot of $\ln [I_{oi}/Kf^2]$ versus T is shown in Fig. 1. A feature of the data is the very rapid decrease with temperature of the intensities of all the reflexions between room temperature and the melting point. It has not been possible to fit this high-temperature data, considered separately or with the rest of the data, with any anharmonic model. All fits referred to below were made using only those intensities measured at up to 310 K.

The solid lines shown in Fig. 1 represent plots of $\ln [I_{ci}/Kf^2]$ versus T where the I_{ci} were calculated using the quasiharmonic model for temperature factor. That is, the temperature variation of α due to expansion was taken into account according to equation (2), but the anharmonic parameters γ and δ in the temperature-factor expression (1) were set to zero. An extension to a fully anharmonic temperature-factor expression in the fitting procedure did not give values of γ or δ significantly different from zero for this set of data.

The value of R quoted in Fig. 1 was calculated as

$$R = \frac{\sum_i \omega_i |I_{oi} - I_{ci}|}{\sum_i \omega_i I_{oi}}$$

The value of α_0 obtained from the quasi-harmonic fit is $0.267 \pm 0.024 \text{ eV \AA}^{-2}$ referred to 273 K. A Debye temperature θ_D calculated in the usual way from this result is $140 \pm 6 \text{ K}$ at 273 K. This is in satisfactory agreement with the room-temperature determination of $134 \pm 2 \text{ K}$ reported in I. Other determinations have been $120 \pm 4 \text{ K}$ (Dawton, 1937), $154 \pm 8 \text{ K}$ (Geshko *et al.*, 1968) and $140 \pm 1 \text{ K}$ (Kumar, Valvoda & Viswamitra, 1971). The variation of α , θ_D and the Debye parameter B with temperature is shown in Fig. 2.

Although we have been unable to describe all the high-temperature data in terms of the fourth-order one-atom-potential model for anharmonic temperature factor, an estimate of anisotropy can be made by examining the 330–411 pair of reflexions which occur at the same Bragg angle, and on an isotropic model would be expected to have the same intensity.

Using expression (1) for temperature factor, ignoring the isotropic anharmonic terms, and the harmonic term which cancels, we can write

$$\ln \left[\frac{I_0(330)}{I_0(411)} \right]_T = \ln \left[\frac{\tau^2(330)}{\tau^2(411)} \right] = 192(k_B T)^3 \left(\frac{2\pi}{a} \right)^4 \left(\frac{\delta}{\alpha^4} \right). \quad (4)$$

Values of δ/α^4 have been determined using equation (4) from the ratio of intensities of the 330 and 411 reflexions for the temperature range from 293 to 363 K. Results are plotted in Fig. 3, together with estimated errors. The sign of δ/α^4 is positive as found in the room temperature study (I) but the value at 293 K of 6.8 is about half that of $15.2 \text{ eV}^{-3} \text{ \AA}^4$ found in the original study. On the fourth-order single-atom-potential model used here the interpretation of positive δ/α^4 , contrary to that given in I, is that there is greater probability that the atom will vibrate towards its nearest neighbours in the body-diagonal directions and less that it will vibrate towards its next-nearest neighbours in the cube-axis directions. This is unexpected since core repulsion between atoms might be expected to cause the atoms to vibrate preferentially toward their next nearest neighbours. Positive δ/α^4 values have been found in another crystal recently, SrF_2 , by Mair, Barnea, Cooper & Rouse (1974). However, SrF_2 is highly ionic and Mair *et al.*, consider the anisotropic effect to be due to Coulombic forces between nearest neighbours.

Comparison with theory

Willis (1969) used experimental data on the temperature dependence of diffracted intensities from potassium chloride and an harmonic temperature-factor model derived from lattice-dynamical calculations to estimate the contribution of the anharmonic parameter γ to the data. The same procedure has been used recently by Pathak & Pandya (1975) for potassium iodide and rubidium iodide.

In the case of sodium, calculations for the depen-

dence of the integrated intensities on temperature, based on harmonic lattice-dynamical calculations, have been given over several years by members of a group at the University of Allahabad, India (*e.g.* Prakash, Pathak & Hemkar, 1975; Sangal & Sharma, 1971; Singh & Sharma, 1971; Singh & Sharma, 1969). Their results vary somewhat depending on the model chosen for the calculation. The most recent result of Prakash *et al.* corresponds to a value for α_0 of 0.80 eV \AA^{-2} .

A calculation of $\langle u^2 \rangle$, the mean-square atomic displacement, based on an Einstein approximation, has been given recently by Dobrzynski & Masri (1972). The value for α_0 derived from their calculation is 0.58 eV \AA^{-2} .

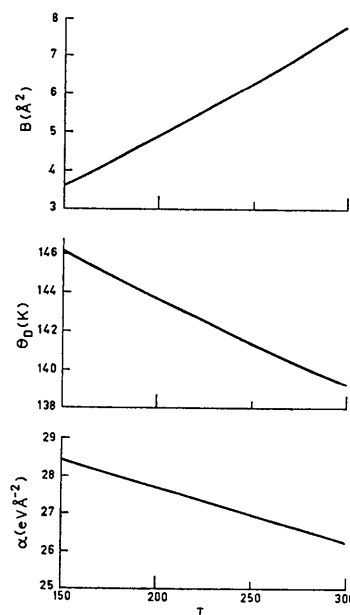


Fig. 2. The variation of B , θ_D and α with temperature T (K). The values of α are multiplied by 100.

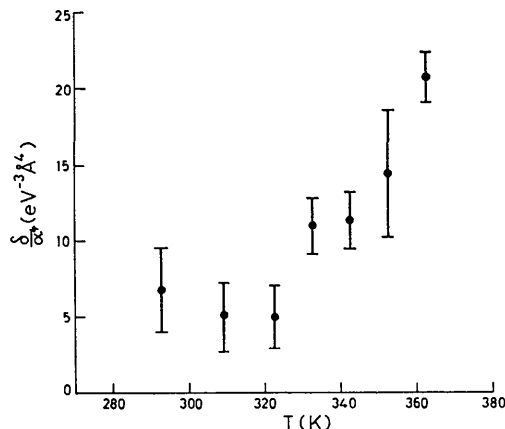


Fig. 3. The variation of δ/α^4 with temperature.

Both these calculated values for α_0 are much larger than the experimental value of $0.267 \text{ eV } \text{\AA}^{-2}$ and the values of γ required to fit the data using the calculated values for α_0 are of too great magnitude to be reasonable.

Discussion

The temperature dependence of the integrated intensities in sodium may be described adequately in terms of a quasi-harmonic model for the temperature factor in the temperature range 148 K to about room temperature.

The rapid decrease in the integrated intensities from room temperature to the melting point, and the anisotropy observed, cannot be described by the simple anharmonic model for temperature factor used here. It is interesting that these effects occur in the same temperature range in which defects become important. Feder & Charbneau (1966) measured the length and lattice-parameter expansion of sodium with temperature. The two curves begin to diverge at $\sim 300 \text{ K}$ and reach a relative difference of $\sim 4\%$ at the melting point. Feder *et al.* show that sodium has a high net vacancy concentration of 7.5×10^{-4} and a very low vacancy migration energy of $0.03 \pm 0.03 \text{ eV}$ at the melting point, which indicates a very rapid vacancy migration at temperatures near the melting point. They conclude that the best description of their results is in terms of a relaxation of the lattice in the region surrounding the vacancy, based on the model of Nachtrieb & Handler (1954). Recently Torrens & Gerl (1969) have carried out a computer-simulation investigation of diffusion mechanisms in the alkali metals. They conclude that it is necessary to consider in their calculation at least five shells of atoms in the relaxation area around the vacancy, and that the relaxation is strongly anisotropic, being greatest in the $\langle 111 \rangle$ directions, with nearest-neighbour displacements being about 8% , *i.e.* about 0.3 \AA .

This relaxation model for a region around a vacancy coupled with a high vacancy concentration and mobility, could account qualitatively for the observed behaviour of the integrated intensities in sodium. The relaxation process would distort the average single-atom potential considerably as the vacancy concentration increased, which may account for the rapid decrease in intensity of all reflexions with temperature, and the strong anisotropy of the relaxation and recovery as the vacancy passed through a section of the lattice may account for the observed anisotropy in the intensity with an apparent greater probability of

motion in the body-diagonal directions. Both these effects would depend on the vacancy concentration, which is exponential, rather than on an integral power of the temperature. This may explain the rapidity of the variation of the effects with temperature.

We note here also that Jackson, Powell & Dolling (1975) have used experimental phonon frequency distributions for the b.c.c. elements molybdenum and niobium to show that there are correlations of motions of atoms in the lattice which increase with temperature and which are greatest in the $\langle 111 \rangle$ directions.

This work was supported in part by the Australian Research Grants Committee.

References

- DAWTON, R. H. V. M. (1937). *Proc. Phys. Soc.* **49**, 294–306.
 DOBRZYNSKI, L. & MASRI, P. (1972). *J. Phys. Chem. Solids*, **33**, 1603–1609.
 DOYLE, P. A. & TURNER, P. S. (1968). *Acta Cryst.* **A24**, 390–397.
 FEDER, R. & CHARBNAU, H. P. (1966). *Phys. Rev.* **149**, 464–471.
 FIELD, D. W. & MEDLIN, E. H. (1974). *Acta Cryst.* **A30**, 234–238.
 FRITSCH, G., GEIPEL, F. & PRASETYO, A. (1973). *J. Phys. Chem. Solids*, **34**, 1961–1969.
 GESHKO, E. I., KUSHTA, G. P. & MIK'HALCHENKO, V. P. (1968). *Ukr. Fiz. Zh.* **13**, 1788–1792.
 JACKSON, D. P., POWELL, B. M. & DOLLING, G. (1975). *Phys. Lett.* **51A**, 87–88.
 KUMAR, S. K., VALVODA, V. & VISWAMITRA, M. A. (1971). *Curr. Sci.* **40**, 459–460.
 MAIR, S. L., BARNEA, Z., COOPER, M. J. & ROUSE, K. D. (1974). *Acta Cryst.* **A30**, 806–813.
 MARTINSON, R. H. (1969). *Phys. Rev.* **178**, 902–913.
 NACHTRIEB, N. H. & HANDLER, G. S. (1954). *Acta Met.* **2**, 797–802.
 PATHAK, P. D. & PANDYA, N. M. (1975). *Acta Cryst.* **A31**, 185–188.
 PRAKASH, J., PATHAK, L. P. & HEMKAR, M. P. (1975). *Aust. J. Phys.* **28**, 63–68.
 ROUSE, K. D. & COOPER, M. J. (1969). *Acta Cryst.* **A25**, 615–621.
 SANGAL, S. K. & SHARMA, P. K. (1971). *Z. Phys. Chem. Liepz.* **247**, 257–264.
 SIEGEL, S. & QUIMBY, S. L. (1938). *Phys. Rev.* **54**, 76–78.
 SINGH, A. K. & SHARMA, P. K. (1969). *J. Phys. Soc. Japan*, **26**, 425–431.
 SINGH, N. & SHARMA, P. K. (1971). *Phys. Rev.* **B3**, 1141–1148.
 TORRENS, I. M. & GERL, M. (1969). *Phys. Rev.* **187**, 912–924.
 WILLIS, B. T. M. (1969). *Acta Cryst.* **A25**, 277–300.
 WILLIS, B. T. M. & PRYOR, A. W. (1975). *Thermal Vibrations in Crystallography*. Cambridge Univ. Press.